Applied Acoustics 206 (2023) 109321

Contents lists available at ScienceDirect

Applied Acoustics

journal homepage: www.elsevier.com/locate/apacoust

Quasi-perfect and wideband absorption with gradient non-uniform micro-slit array absorber via a hierarchical optimization method

Weiwei Liao, Run Hu, Guanying Xing, Xiaobing Luo *

School of Energy and Power Engineering, Huazhong University of Science and Technology, Wuhan 430074, China

ARTICLE INFO

Article history:
Received 1 November 2022
Received in revised form 1 February 2023
Accepted 7 March 2023

Keywords:
Transfer matrix method
Visco-thermal analysis
Multi-objective genetic algorithm optimization
Quarter-wavelength resonator

ABSTRACT

Gradient micro-slit array absorber, a kind of acoustic metamaterial, made of multiple quarter-wavelength resonators, is holding a promising future in industrial utilization due to its flexible adaptation and simple structure. However, designing a perfect and broadband absorber remains a huge challenge because of the larger number of the design parameters and complicated coupling effect between different resonators. In this study, a hierarchical optimization method is developed for gradient micro-slit array absorber. First, a prior test based on two-slit absorber is conducted using transfer matrix method (TMM) to give directions on designing a multi-slit absorber. And then an original absorber model is constructed in the range of 1000–1800 Hz. For the first step, the optimal width of the slit is obtained through the analysis of the quality factor. For the second step, the spacings between slits is optimized by maximizing absorption and minimizing the total length of the waveguide. After optimization, the absorption performance of the optimized model increased by 15.6% and the length decreased by 46% compared with the original model. Finally, the gradient micro-slit array absorber is experimentally investigated and achieves a quasi-perfect and flat absorption ranging from 1000 Hz to 1800 Hz.

1. Introduction

Noise pollution has been an annoying problem, which will induce insomnia, headache, and many other health problems for humans if not handled properly. Traditional noise reduction materials such as porous materials are very limited because their low frequency lies in the inertial regime[1], meaning that the structure thickness needs to be comparable to its working wavelength to achieve high absorption. Alternatively, acoustic metamaterials, which are made of periodic subwavelength structures, are qualified to absorb sound energy with a relatively smaller size. In terms of the type of unit cell, acoustic metamaterials can be divided into three categories: Helmholtz resonator[2–5], quarter-wavelength resonator(QWR)[6–8](when the channel is one-quarter wavelength, it's called Fabry-Perot resonator[9–13]) and membrane-type resonator[14–16]. Nevertheless, a single resonator usually possesses a narrow absorption band[17], which is unsuitable for practical application. To acquire perfect and broadband absorption, overlapping of resonances[3,18–20], accumulation of resonances through strong dispersion[21], transition of the resonator's boundary from solid to soft[22,23] and utilization of high-order resonances[24,25] are all effective approaches, among which overlapping of resonances stands out in a direct and efficient manner. Table1.

Gradient micro-slit array absorber is a combination of different quarter-wavelength resonators that takes advantage of overlapping of resonances to form broadband absorption. When compared with other well-established absorbers like micro-perforated plates, it stands out with excellent reliability because the simple structure of resonator guarantee that it won't be blocked by the floating particle in the air. Moreover, its adjustability is reflected in the property that its operating frequency is directly related to its length of the resonator cavity, so it's full of potential to be applied in industrial noise reduction. Yet it features the growing number of design parameters with the target absorption frequency band widening. Apart from that, the coupling between adjacent resonators can't be neglected. Therefore, it's intractable to design a perfect and broadband absorber. To maximize the overlapping of resonances of the different QWRs, most work still either simply connect several discrete resonances[24] which induce dips in absorption spectra inevitably, or adopt porous material to broaden the frequency band[7,26] which will induce the unreliability for practical application, or adopt deep learning method[27] which will certainly cost tremendous time to acquire training data, which is unsuitable in real situation.

* Corresponding author.
E-mail address: luoxb@hust.edu.cn (X. Luo).

https://doi.org/10.1016/j.apacoust.2023.109321
0003-682X/

Hence, it's crucial to develop a design method for gradient micro-slit array absorber to achieve high and broadband absorption. In this work, a hierarchical optimization method based on genetic algorithm is proposed to design a gradient micro-slit array absorber to achieve perfect and broadband absorption. Without losing generality, we focus on the frequency ranging from 1000 to 1800 Hz as a demonstration. The transfer matrix method is modified by the visco-thermal effect to accurately simulate the gradient micro-slit array absorber. Firstly, a prior test based on a two-slit absorber is conducted where three dimensional parameters are explicitly studied to identify their separate influence on the total absorption performance. The prior test provides guidance for the next design and optimization procedures. For the first step, the width of the slit is carefully selected because of its close relation to the visco-thermal effect. For the second step, multi-objective genetic algorithm is adopted to optimize the spacing of the slits and total length of the absorber simultaneously. In result, the overall performance is greatly enhanced by 15.6% and the length is reduced by 46% compared with the original case. The optimization performance is verified by the complex frequency plane method. Finally, the absorber composed of twenty gradient non-uniform slits is fabricated and exhibits quasi-perfect and wideband absorption in 1000–1800 Hz through experimental validation, demonstrating the effectiveness of the hierarchical optimization method.

2. Gradient micro-slit array absorber

Gradient micro-slit array absorber consists of an array of slit resonators which arrange in a line. The mechanism of sound absorption of a slit resonator can be summarized as: sound energy dissipates in the form of the standing wave in a quarter-wavelength slit. The relation between the slit height and the wavelength can be expressed as follow:

$$h = \frac{(2k+1)}{4}\lambda, k \in N \tag{1}$$

where k is the wavenumber, λ is the wavelength. When the depth of the slit is an odd number integer multiple of the quarter wavelength, the sound wave would be trapped in the slit, which is also the mechanism of the intriguing phenomenon- rainbow trapping [24,28].

2.1. Theoretical modeling

Transfer matrix method(TMM)[29,30] is one of the efficient and accurate methods to model the different kinds of acoustic metamaterials. The visco-thermal analysis is introduced to accurately predict the absorption performance of the gradient micro-slit array absorber. The width of the slit is usually of the order of millimeters. Therefore, the visco-thermal effect is nonnegligible when acoustic waves propagate in the slits, especially when the thermal and viscous boundary layer thickness (calculated by Eqs. (2) and (3)) is comparable with the slit dimension.

$$\delta_{visc} = \sqrt{\frac{2\mu}{\omega\rho_0}} \tag{2}$$

$$\delta_{therm} = \sqrt{\frac{2\kappa}{\omega\rho_0 C_p}} \tag{3}$$

where μ is the viscosity of the air, κ is the thermal conductivity of the air, C_P is the heat capacity of the air, and ω is the radian frequency of the sound.

Acoustic energy loss occurs in the process of propagation, which is the mechanism of sound absorption. Considering the loss during the transmission, the effective density and effective bulk modulus take the following forms.

$$\rho_f(\omega) = \rho_0\left[1 - \frac{tanh\frac{d}{2}G_\rho(\omega)}{\frac{d}{2}G_\rho(\omega)}\right]^{-1} G_\rho(\omega) = \sqrt{\frac{i\omega\rho_0}{\eta}} \tag{4}$$

$$K_f(\omega) = K_0[1 + (\gamma-1)\frac{tanh\frac{d}{2}G_k(\omega)}{\frac{d}{2}G_k(\omega)}]^{-1} G_k(\omega) = \sqrt{\frac{i\omega Pr\rho_0}{\eta}} \tag{5}$$

where ρ_0 is the density of air, K_0 is the bulk modulus of air, d is the width of slit, Pr represents Prandtl number, η represents the dynamic viscosity of air.

The impedance and the wave number can be obtained according to the above two characteristic parameters,

$$k_f = \omega/\sqrt{\frac{K_f}{\rho_f}} \tag{6}$$

$$Z_f = \sqrt{K_f\rho_f} \tag{7}$$

Once the impedance and the wave number are obtained, the effective impedance of the micro-slit array resonator can be expressed as,

$$Z_{slit} = -i\frac{Z_f}{S_f}\cot(k_f l) - i\omega\rho_0\frac{\Delta l}{S} \tag{8}$$

$$\Delta l = 0.82[1 - 0.235\frac{r_n}{r_t} - 0.132\left(\frac{r_n}{r_t}\right)^2 + 1.54\left(\frac{r_n}{r_t}\right)^3 - 0.86(\frac{r_n}{r_t})^4]r_n \tag{9}$$

where S_f is the section area of the slit, l is the height of the slit, Δl is the correction term, r_n is the radius of the loaded waveguide and r_t is the radius of the main waveguide, and S is the section area of the main waveguide.

The slit is laterally mounted to the main wave guide, so the transfer matrix is

$$T_{slit} = \begin{bmatrix} 1 & 0 \\ 1/Z_{slit} & 1 \end{bmatrix} \tag{10}$$

The transfer matrix of the tube used for connect the two neighboring slits is

$$T_{tube} = \begin{bmatrix} \cos(k\delta) & \frac{iZ_0}{h}\sin(k\delta) \\ i\frac{h}{Z_0}\sin(k\delta) & \cos(k\delta) \end{bmatrix} \tag{11}$$

δ is the spacing between two neighboring slits.

Considering n slits array, the total transfer matrix is

$$\mathrm{T}_{total} = (\mathrm{T}_{slit} * \mathrm{T}_{tube} * \mathrm{T}_{slit})^{n-1} \tag{12}$$

Assuming that the absorber is one-port and there is no transmission, the reflection is calculated in the following equation

$$R = \frac{T_{total}(1,1) - Z_0/ST_{total}(2,1)}{T_{total}(1,1) + Z_0/ST_{total}(2,1)} \tag{13}$$

And the absorption rate can be expressed as:

$$\alpha = 1 - |R|^2 \tag{14}$$

2.2. Optimization method

In terms of gradient micro-slit array absorber, there are multiple parameters to be optimized and the number of the optimized

parameters is growing with the number of slits growing. Genetic algorithm takes example from the natural selection, mutation and evolution process in biotic population, which is suitable for this kind of complex problem. Here, the evaluation index(shown in equation(15)) is equal to the absorption coefficient integral on the specified frequency range, which both consider the magnitude and width of the absorption spectra. The integral frequency resolution is set to 2.

$$I = \int_{f_1}^{f_2} \alpha(f) df \tag{15}$$

where α denotes the absorption rate, f_1 and f_2 represent the lower and upper limit of the integral respectively. To design a perfect absorber, it's not only excellent absorption that is needed but also the smallest possible dimension for practical application. Therefore, we set two objectives that conflict with each other: minimize the total length of the waveguide of the absorber and maximize the absorption integral on the interested frequency. After optimization, the result of data points form a pareto front among which a certain data point is chosen according to practical demand.

2.3. Experimental measurement

The impedance tube method is broadly adopted to test the absorption of all kinds of material. Herein, the B&K 4206 type is used and the two microphones method based on ASTM-E1050 [31] is utilized. A digital signal generated by the computer is sent to the power amplifier and then powered the loudspeaker. By analyzing the two microphones' electric signals, a transfer matrix is available. The reflection rate can be calculated as follow,

$$R = |R|e^{j\varphi R} = R_r + jR_i = \frac{H - e^{-jks}}{e^{jks} - H} e^{j2k(l+s)} \tag{16}$$

where l represents the distance between the absorber and the nearest microphone, s represents the distance between the two microphones, and H represents the transfer matrix between the two microphones. Once the reflection rate is obtained, the absorption rate of the measured specimen can be calculated.

3. Results and discussions

3.1. Priori test

Generally speaking, there exists coupling effect between adjacent slits in a micro-slit array absorber. The acoustic wave localization is a synthetical consequence induced by the acoustical oscillation in a single slit and the near-field coupling among the neighboring slits. And the coupling is controlled by the diffracted evanescent waves, making the pressure and velocity fields oscillate in opposite phases in adjacent slits[28]. Hence, a combination of two slits can be treated as a basic unit as illustrated in Fig. 1. To manifest how the dimensional parameters of the slits array influence the overall absorption, an example of two slits is discussed, which have different lengths and identical widths and are separated by the distance of$d$ >0.

According to the TMM theory, the reflection can be simplified into the following form,

$$R = \frac{(1 - Z_1)(1 - Z_2)(\cos(kd) - i\sin(kd)) - \cos(kd)Z_1Z_2 - i\sin(kd)Z_1}{(1 + Z_1)(1 + Z_2)(\cos(kd) + i\sin(kd)) - \cos(kd)Z_1Z_2 - i\sin(kd)Z_1} \tag{17}$$

Z_1 and Z_2 are the normalized impedance of the first and second slit resonator respectively, which can be obtained by Eq. (8). The impedance of the slit resonator is mainly related to these two

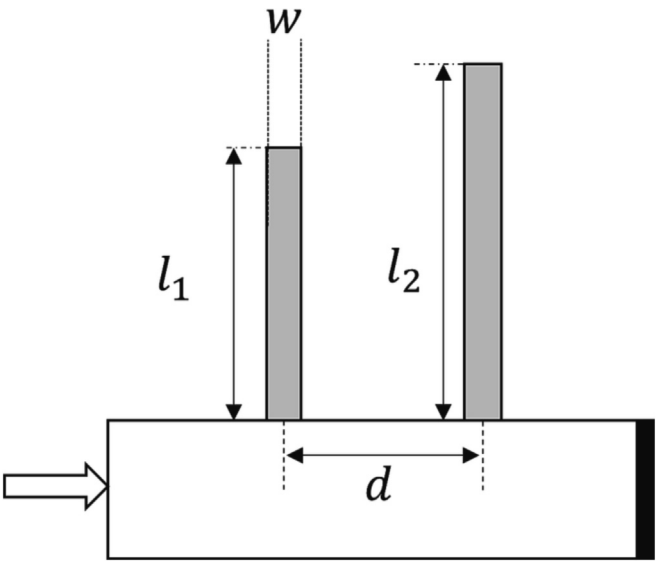

Fig. 1. A one-port two-slit absorber.

parameters, the slit height l and the slit width w. As can be seen from Eq. (17), the reflection rate R is related to multiple parameters l_1, l_2, w and d at a certain frequency.

The relative length of the two slits on the overall sound absorption is firstly explored. Except for these two parameters, l_1 and l_2, the rest parameters are fixed. The impedance Z_1 and Z_2 range from 3 to 10 and the variation of value R over Z_1 and Z_2 is shown in Fig. 2a. As is illustrated in Fig. 2a, in the region of $Z_2 < Z_1$, R is smaller than R in the region of $Z_2 > Z_1$. Therefore, to get larger absorption, Z_2 needs to be smaller than Z_1. Furthermore, because the impedance Z is proportional to the cot(kl), and cot(x) is monotonically decreasing in the interval of [0, pi]. As a result, it's beneficial to set l_2 greater than l_1, indicating that the length of the slit should be gradually increasing to get larger absorption.

Next, l_1 and l_2 are set unchanged, and by changing the spacing between slits, a curve is obtained shown in Fig. 2b. As shown in this figure, in the range of 0–0.005 m, R descends sharply with the value d increasing and then ascends slowly in the range of 0.01–0.03 m. The results show that the value d is significantly related to the reflection as it can modulate the overall impedance of the micro-slit array absorber. The closer the impedance of the absorber is to the air, the smaller the reflection rate.

Finally, the effect of the width is explored. Generally, the width can neither be too large to absorb sound energy because the viscothermal effect will be weakened, nor too small because it will aggravate the impedance mismatch between the slit and the air. As shown in Fig. 2c, with increasing of w, the value R first descends and then ascends, the tendency of which is just as speculated.

In summary, in terms of a micro-slit array absorber, the length should be gradually increasing alongside the wave propagation direction and the spacings and the widths of the slits ought to be carefully modulated to get a satisfying absorption performance.

3.2. Parametric optimization

The separation of parameters of the design process is based on the concept that the length of the loaded waveguide determines the resonant frequency, the width determines the overlapping effect, namely the smoothness between the resonant peaks and the distance between slits determine the acoustical reflection. The three key parameters separately determine different characters of the slits resonators and their mutual coupling effect is

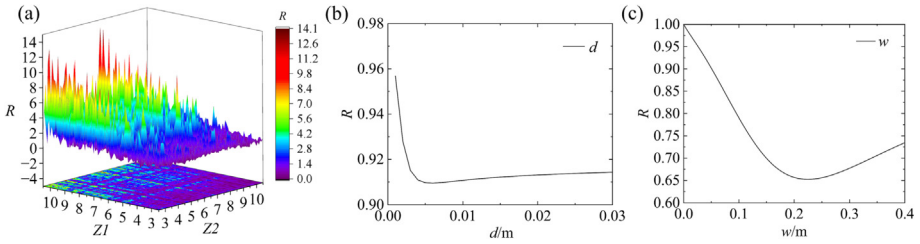

Fig. 2. (a) Change of reflection rate versus the two slits' impedance. (b) Change of reflection rate versus distance between the adjacent slits. (c) Change of reflection rate versus the slit width.

viewed as weak so we can design it separately. Thus, the design process is accordingly divided into 3 steps and the first two steps is aimed at l and w, and the last step is aimed at improving compactness.

3.2.1. Original model

To fulfill the demand of perfect absorption in the range of 1000–1800 Hz, a gradient micro-slit array absorber consisting of 20 slits is constructed shown in Fig. 3a. The lengths are evenly distributed from h_1 = 43 mm to h_{20} = 81 mm with an increase of dh = 2 mm. The diameter of the main waveguide is 29 mm. The absorption performance of the original case is simultaneously simulated by TMM and COMSOL. And the comparative result is shown in Fig. 3b, the simulated result coincides with each other, indicating that numerical model built by TMM is accurate enough to serve as the surrogate model. The absorption spectrum is shown in Fig. 3b and the overall absorption integral is 689.2. With frequency increasing, the absorption performance grows worse. Concretely speaking, the overlapping between resonances gets weaker as frequency increases.

3.2.2. Quality factor and optimal width

The overlapping between resonances can be determined by the quality factor which is defined by Eq. (18).

$$Q^{-1} = \frac{\Delta f}{f_r} = Q_{loss}^{-1} + Q_{leak}^{-1} \tag{18}$$

where Δf is the width of the frequency band, f_r is the resonant frequency. The quality factor of a resonance consists of two terms: Q_{loss}^{-1} and Q_{leak}^{-1}, the former of which is related to the loss caused by the visco-thermal effect, the latter of which is used to measure the acoustic energy leakage from the resonator to the external space. Decreasing the quality factor can enhance the overlapping effect, which contributes to broadband absorption[1]. The reflection rate can be expressed as follow,

$$r = 1 - \frac{2Q_{leak}^{-1}}{-2i\left(\frac{f}{f_r} - 1\right) + Q_{loss}^{-1} + Q_{leak}^{-1}} \tag{19}$$

According to Eqs. (18) and (19), Q_{leak}^{-1} and Q_{loss}^{-1} can be calculated. The minor adjustment of the slit length compensates for the variation of resonant frequency caused by the change of slit width. With width variated from 1 mm to 5 mm, 5 sets of data points can be obtained shown in Fig. 3c.

From Fig. 3c, the variation tendency of Q_{loss}^{-1} is as speculated, decreasing with slit width increasing. Moreover, the loss factor dominates the quality factor, and Q^{-1} is gradually decreasing due to the increasement of the slit width. It can be concluded that the slit width is the key factor that influences the quality factor of the resonance. To fulfill the requirement of broadband, the micro-slit array absorber can be optimized by decreasing the slit width for a stronger visco-thermal effect, thus increasing the loss factor(Q_{loss}^{-1})[32]and then leading to greater overlapping between

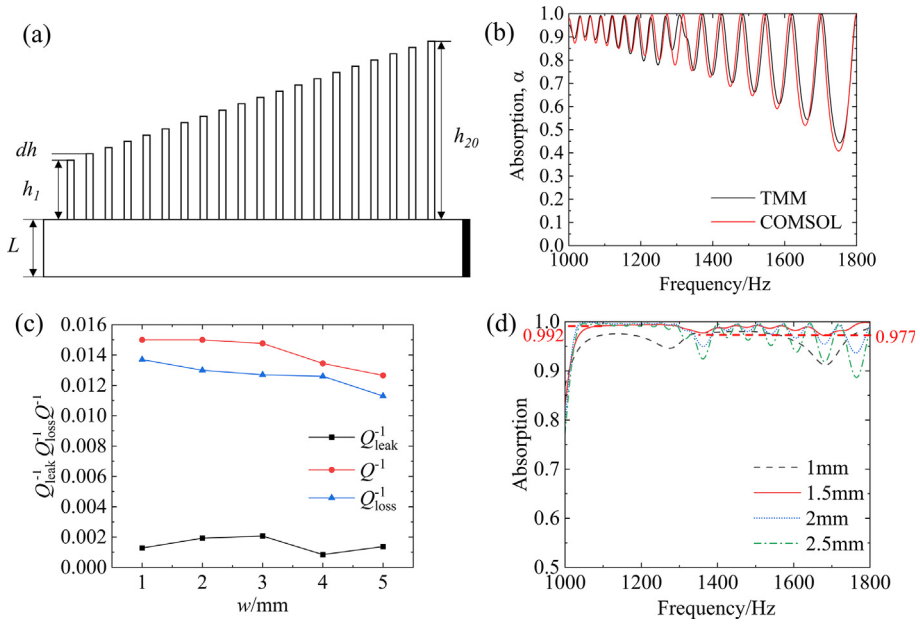

Fig. 3. (a)Schematic of the gradient slits array absorber designed by experience. (b) Absorption spectra of the aforementioned absorber calculated by the COMSOL and TMM respectively. (c) Variation of the quality factors curves versus slit width of the single slit absorber. (d) Absorption spectrum of absorbers of different slit widths.

resonances. Hence, the absorption integral is studied within the interval of 0.5–3 mm.

From Fig. 3d, the optimal width is 1.5 mm, and the narrower the slit width is not the better. The reflection grows larger when the slit gets narrower because it gets harder for acoustic waves to propagate into the slit due to the impedance mismatch between the slit and the environment. The optimal absorption integral over the frequency range is 775.9, which is fairly high but there is still room for improvement, as there's still little fluctuation of the absorption curve in the range of 1350–1800 Hz as illustrated by Fig. 3d. And nearly all resonances don't reach a perfect absorption state, indicating that decreasing width can improve the overlapping effect and then promote broadband, but impairs the absorption effect. To solve this problem, work can be done from the aspect of the spacing optimization of the micro-slit array absorber.

3.2.3. Multi-objectives GA optimization

In order to get a perfect and broadband absorption and improving the compactness at the same time, multi-objectives GA optimization is introduced into the design process. Since the gradient slits array absorber is made up of 20 slits, there are 19 parameters to be optimized. The whole optimization process takes about half an hour. After optimization, we get 70 data points which constitute the Pareto front shown in Fig. 4a. In the end, the data point (796.7, 0.0962) is picked after giving an overall consideration to the trade-off between the absorption and the dimension. When compared with the original case, the absorption integral increased by 15.6% and the length decreased by 46%.

The optimized results are listed in Table1, and the 3-D model shown in Fig. 4b is built based on the optimized results.

3.3. Complex frequency plane analysis method

Complex frequency plane analysis method is a useful method that provide rich and important information about each of a resonance of the absorber, also providing useful insights for the design of absorbers[1,33,34]. Each pair of a zero(shown in blue dot in Fig. 5a and b) and a pole(shown in red dot in Fig. 5a and b) represents a resonance, the distance between the zero and pole indicates the magnitude of the quality factor. When the absorber is lossless, the absorber is subjected to leakage, and the zeros and poles of the reflection is symmetric about the real frequency axis. When Q_{loss}^{-1} is introduced into the system, the zeros and poles move upwards as a whole. When zeros reach the real frequency axis, it indicates that the resonance reaches a perfect absorption state. Therefore, it's a powerful tool to design perfect absorbers in acoustics.

By substituting the frequency term into a complex form in the TMM model, a complex frequency plane can be obtained as shown in Fig. 5. From Fig. 5a, the original slits array absorber's zeros all deviate a little from the real axis, indicating that few resonances reach a perfect absorption state. In addition, each resonance's poles and zeros are quite close, indicating a poor overlapping effect, to the disadvantage of broadband absorption.

After optimization, as illustrated in Fig. 5b, zeros move upwards as a whole, indicating that each resonance isn't perfect. But there still form perfect and flat absorption spectra, further confirming that coupled weak resonances could form a wide absorption frequency range[35]. And the distance between poles and zeros of the resonances gets large in the range of 1400–1600 Hz, promoting broadband absorption.

In conclusion, from the comparison between the original case and the optimized case, we can conclude that the optimization greatly promotes the overlapping effect and enhances the absorption performance, making it possible to form a perfect and broadband absorption.

3.4. Experimental validation

The measured specimen is fabricated by 3D printing technology, and the manufacturing precision is 0.1 mm, which is qualified for engineering application. Because the specimen is not a regular shape like a cube or cylinder, the specimen can only be mounted outside as depicted in Fig. 6a, connected by a self-made connector

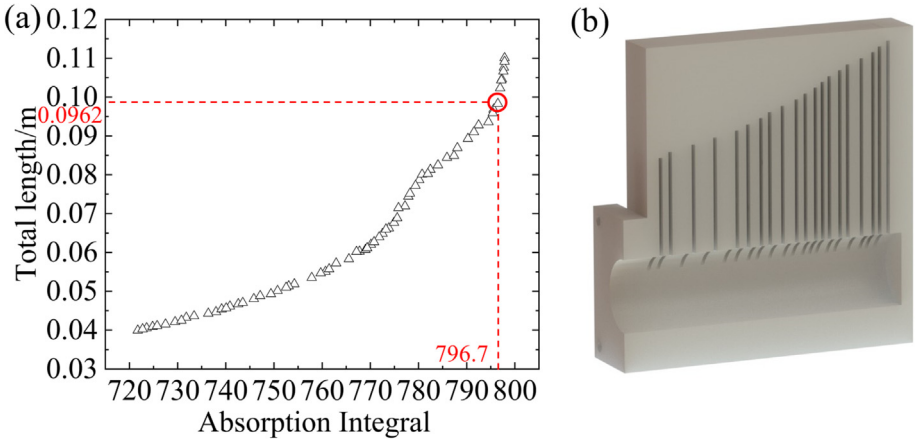

Fig. 4. (a) Pareto front. (b) The cross-section diagram of the 3-D model of the optimized absorber.

Table1
Optimized spacings between slits.

Number	1	2	3	4	5	6	7	8	9	10
Dimension(mm)	4	9.7	9	9.2	4.7	5.5	3.7	5.4	5.9	3.8
Number	**11**	**12**	**13**	**14**	**15**	**16**	**17**	**18**	**19**	
Dimension(mm)	4.3	3	2.9	4.5	3.3	5.9	5	2.8	3.6	

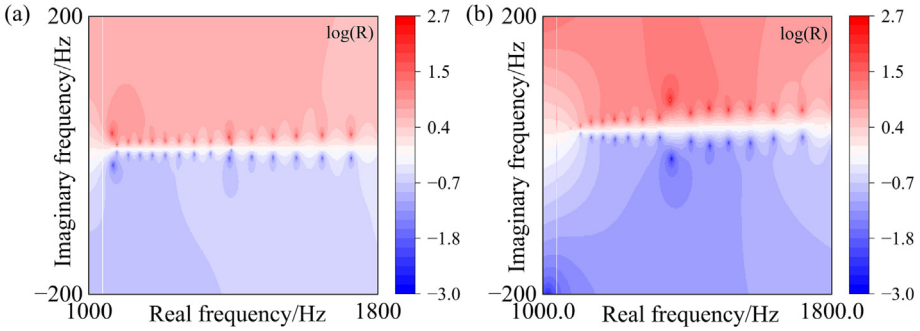

Fig. 5. Complex frequency plane comparison between (a) the original model and (b) the optimized model.

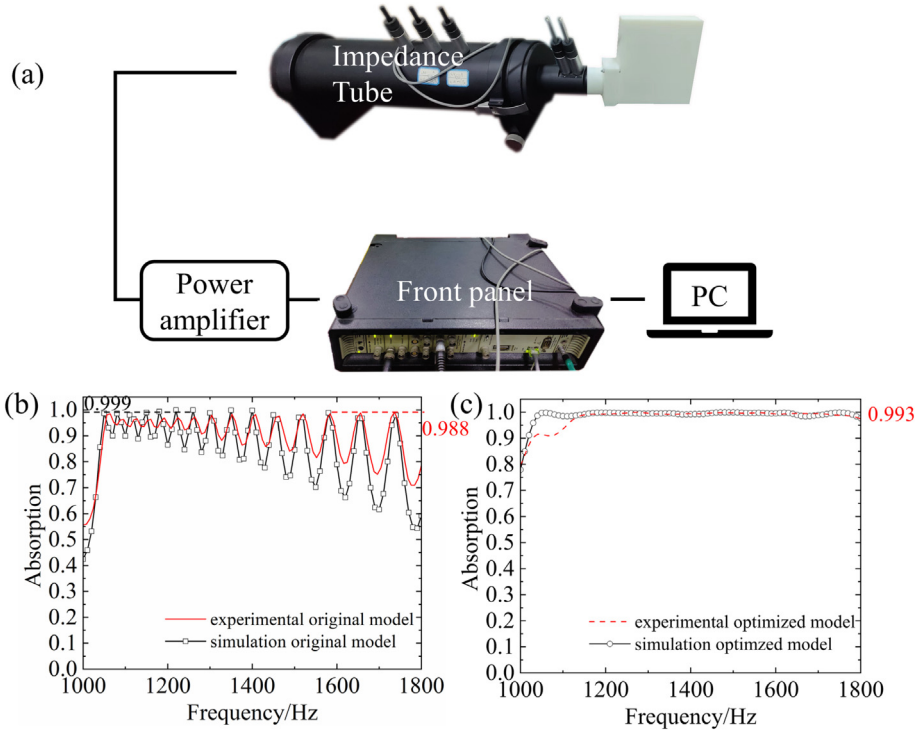

Fig. 6. (a) Experimental measurement setup. (b) Experimental and simulation results of the original model. (c) Experimental and simulation results of the optimized model.

to the speaker tube. Extra sound insulation measures should be carried out to prevent the sound leakage from the connection.

The measured acoustic behavior of the original and optimized gradient slits array is presented in Fig. 6b and c respectively. As shown in Fig. 6b, the black rectangular-dot line and the red solid line represent the numerical simulated and the experimental result of the original absorber respectively, nearly all the characteristic absorption peak is identical except a little deviation in amplitude. And the deviation is growing large as the frequency increases. This might be caused by the sound leakage from the connection, which goes up with the wavelength reducing and this part of energy is counted as being absorbed. Both experimental and simulation results show that the fluctuation grows intense as the frequency increase, because the higher frequency resonance showcases thinner viscous and thermal boundary, leading to weaker visco-thermal effect and weaker overlapping effect. Further, the black circular-dot line and the red dash line represent the numerical simulated and the experimental result of the optimized absorber respectively in Fig. 6c. And they are very consistent, which is flat and up to 1 in the studied frequency range, demonstrating that the effectiveness of the hierarchical optimization method.

It can be concluded that narrower slits contribute to forming a broadband absorption by promoting the visco-thermal effect. In addition, the appropriate distribution of the spacings between the micro-slit is necessary to suppress the sound reflection with the impedance match with the air, which can further increase the absorption rate. Appling the hierarchical optimization method, a quasi-perfect and wideband gradient non-uniform micro-slit array absorber can be obtained by maximally promoting the overlapping of resonances and the impedance match.

If the absorption frequency range is extended to lower frequency, the length of the resonator should accordingly increase because the slits resonator is a combination of a series of quarter-wavelength resonator intrinsically. The whole design workflow is applicable in any other operating frequency range.

4. Conclusion

In this work, a hierarchical optimization method is proposed for gradient micro-slit array absorber. Through the prior test, we have theoretically illustrated the necessity to arrange the length of the

slit increasingly. And the importance of the width of the slit to the overlapping effect of the resonances is proven, which is the key point to forming a broadband absorption. Moreover, the spacings of the slits are optimized by genetic algorithm, improving the overall absorption performance by 15.6% and decreasing the length of the absorber by 46% compared with the original model. Eventually, the gradient non-uniform micro-slit array absorber is fabricated and measured by the experiment based on an impedance tube and the absorption spectrum is quasi-perfect and flat ranging from 1000 to 1800 Hz. The great enhancement of the absorption performance suggests the feasibility of the hierarchical optimization method. Furthermore, this method can be transplanted to design a perfect and broadband absorber operating in any other frequency range, providing great convenience for any scenario where noise reduction technology is required.

In practical situations, acoustic waves are coming from all the directions, and the absorption performance depends on the acoustic wave incidence angle. This part of work is worthy of exploration and intended to be carried out in the future research.

CRediT authorship contribution statement

Weiwei Liao: Conceptualization, Methodology, Investigation, Software, Validation, Formal analysis, Data curation, Writing – original draft, Visualization. **Run Hu:** Conceptualization, Methodology, Investigation, Resources, Supervision. **Guanying Xing:** Data curation, Writing – review & editing. **Xiaobing Luo:** Conceptualization, Writing – review & editing, Supervision, Project administration, Funding acquisition.

Data availability

Data will be made available on request.

Declaration of Competing Interest

The authors declare that they have no known competing financial interests or personal relationships that could have appeared to influence the work reported in this paper.

Acknowledgements

This work was supported by Open Fund of Science and Technology on Thermal Energy and Power Laboratory (No. TPL 2019B03).

References

[1] Jiménez N, Umnova O, Groby J-P, editors. Acoustic Waves in Periodic Structures, Metamaterials, and Porous Media: From Fundamentals to Industrial Applications. vol. 143. Cham: Springer International Publishing. 2021. https://doi.org/10.1007/978-3-030-84300-7.
[2] Wu L, Zhai Z, Zhao X, Tian X, Li D, Wang Q, et al. Modular Design for Acoustic Metamaterials: Low-Frequency Noise Attenuation. Adv Funct Mater 2022;32(13):2105712.
[3] Liu CR, Wu JH, Ma F, Chen Xu, Yang Z. A thin multi-order Helmholtz metamaterial with perfect broadband acoustic absorption. Appl Phys Express 2019;12(8):084002.
[4] Guo J, Zhang X, Fang Y, Jiang Z. Wideband low-frequency sound absorption by inhomogeneous multi-layer resonators with extended necks. Compos Struct 2021;260:. https://doi.org/10.1016/j.compstruct.2020.113538113538.
[5] Jena DP, Dandsena J, Jayakumari VG. Demonstration of effective acoustic properties of different configurations of Helmholtz resonators. Appl Acoust 2019;155:371–82. https://doi.org/10.1016/j.apacoust.2019.06.004.
[6] Cavalieri T, Cebrecos A, Groby J-P, Chaufour C, Romero-García V. Three-dimensional multiresonant lossy sonic crystal for broadband acoustic attenuation: Application to train noise reduction. Appl Acoust 2019;146:1–8.
[7] Boulvert J, Humbert T, Romero-García V, Gabard G, Fotsing ER, Ross A, et al. Perfect, broadband, and sub-wavelength absorption with asymmetric absorbers: Realization for duct acoustics with 3D printed porous resonators. J Sound Vib 2022;523:116687.
[8] Shen C, Liu Y, Huang L. On acoustic absorption mechanisms of multiple coupled quarter-wavelength resonators: Mutual impedance effects. J Sound Vib 2021;508:. https://doi.org/10.1016/j.jsv.2021.116202116202.
[9] Long H, Shao C, Cheng Y, Tao J, Liu X. High absorption asymmetry enabled by a deep-subwavelength ventilated sound absorber. Appl Phys Lett 2021;118(26):263502.
[10] Cai X, Xiao J, Zhang H, Zhang Y, Hu G, Yang J. Compact acoustic double negative metamaterial based on coexisting local resonances. Appl Phys Lett 2018;113(24):244101.
[11] Gebrekidan SB, Hwang Y-I, Kim H-J, Song S-J. Broadband impedance matching using acoustic metamaterial with a helical hole. Appl Phys Lett 2019;115(15):151901.
[12] Li X-J, Xue C, Fan Li, Zhang S-y, Chen Z, Ding J, et al. Simultaneous realization of negative group velocity, fast and slow acoustic waves in a metamaterial. Appl Phys Lett 2016;108(23):231904.
[13] Shen Y, Yang Y, Guo X, Shen Y, Zhang D. Low-frequency anechoic metasurface based on coiled channel of gradient cross-section. Appl Phys Lett 2019;114(8):083501.
[14] Ma G, Yang M, Xiao S, Yang Z, Sheng P. Acoustic metasurface with hybrid resonances. Nat Mater 2014;13:873–8. https://doi.org/10.1038/nmat3994.
[15] Xu Q, Qiao J, Sun J, Zhang G, Li L. A tunable massless membrane metamaterial for perfect and low-frequency sound absorption. J Sound Vib 2021;493:115823.
[16] Nguyen H, Wu Q, Chen J, Yu Y, Chen H, Tracy S, et al. A broadband acoustic panel based on double-layer membrane-type metamaterials. Appl Phys Lett 2021;118(18):184101.
[17] Fan J, Zhang L, Wei S, Zhang Z, Choi S-K, Song Bo, et al. A review of additive manufacturing of metamaterials and developing trends. Mater Today 2021;50:303–28.
[18] Jiménez N, Romero-García V, Pagneux V, Groby J-P. Rainbow-trapping absorbers: Broadband, perfect and asymmetric sound absorption by subwavelength panels for transmission problems. Sci Rep 2017;7:13595. https://doi.org/10.1038/s41598-017-13706-4.
[19] Ma P-S, Kim H-S, Lee S-H, Seo Y-H. Quasi-perfect absorption of broadband low-frequency sound in a two-port system based on a micro-perforated panel resonator. Appl Acoust 2022;186:. https://doi.org/10.1016/j.apacoust.2021.108449108449.
[20] Boulvert J, Costa-Baptista J, Cavalieri T, Romero-García V, Gabard G, Fotsing ER, et al. Folded metaporous material for sub-wavelength and broadband perfect sound absorption. Appl Phys Lett 2020;117(25):251902.
[21] Jiménez N, Romero-García V, Pagneux V, Groby J-P. Quasiperfect absorption by subwavelength acoustic panels in transmission using accumulation of resonances due to slow sound. Phys Rev B 2017;95:. https://doi.org/10.1103/PhysRevB.95.014205014205.
[22] Ma F, Wang C, Du Y, Zhu Z, Wu JH. Enhancing of broadband sound absorption through soft matter. Mater Horiz 2022;9:653–62. https://doi.org/10.1039/D1MH01685C.
[23] Cui S, Harne RL. Soft Materials with Broadband and Near-Total Absorption of Sound. Phys Rev Appl 2019;12:. https://doi.org/10.1103/PhysRevApplied.12.064059064059.
[24] Jiang X, Liang B, Li R-q, Zou X-y, Yin L-L, Cheng J-C. Ultra-broadband absorption by acoustic metamaterials. Appl Phys Lett 2014;105(24):243505.
[25] Rui Liu C, Hui WJ, Yang Z, Ma F. Ultra-broadband acoustic absorption of a thin microperforated panel metamaterial with multi-order resonance. Compos Struct 2020;246:. https://doi.org/10.1016/j.compstruct.2020.112366112366.
[26] Liu Z, Zhan J, Fard M, Davy JL. Acoustic properties of multilayer sound absorbers with a 3D printed micro-perforated panel. Appl Acoust 2017;121:25–32.
[27] Liu Le, Xie L-X, Huang W, Zhang XJ, Lu M-H, Chen Y-F. Broadband acoustic absorbing metamaterial via deep learning approach. Appl Phys Lett 2022;120(25):251701.
[28] Zhu J, Chen Y, Zhu X, Garcia-Vidal FJ, Yin X, Zhang W, et al. Acoustic rainbow trapping. Acoustic rainbow trapping Sci Rep 2013;3(1). https://doi.org/10.1038/srep01728.
[29] Wang X, Mak CM. Acoustic performance of a duct loaded with identical resonators. J Acoust Soc Am 2012;131(4):EL316. EL322.
[30] Cai C, Mak CM. Acoustic performance of different Helmholtz resonator array configurations. Appl Acoust 2018;130:204–9. https://doi.org/10.1016/j.apacoust.2017.09.026.
[31] E33 Committee. Test Method for Impedance and Absorption of Acoustical Materials Using a Tube, Two Microphones and a Digital Frequency Analysis System. ASTM International. n.d. https://doi.org/10.1520/E1050-12.
[32] Long H, Liu C, Shao C, Cheng Y, Tao J, Qiu X, et al. Tunable and broadband asymmetric sound absorptions with coupling of acoustic bright and dark modes. J Sound Vib 2020;479:115371.
[33] Cheng B, Gao N, Zhang R, Hou H. Design and experimental investigation of broadband quasi-perfect composite loaded sound absorber at low frequencies. Appl Acoust 2021;178:. https://doi.org/10.1016/j.apacoust.2021.108026108026.
[34] Romero-García V, Theocharis G, Richoux O, Pagneux V. Use of complex frequency plane to design broadband and sub-wavelength absorbers. J Acoust Soc Am 2016;139:3395–403. https://doi.org/10.1121/1.4950708.
[35] Huang S, Zhou Z, Li D, Liu T, Wang Xu, Zhu J, et al. Compact broadband acoustic sink with coherently coupled weak resonances. Sci Bull 2020;65(5):373–9.